

Bonding in d 9 complexes derived from EPR: Application to CuCl₂ 4, CuBr₂ 4, and CdCl₂:Cu₂ +

J. A. Aramburu and M. Moreno

Citation: [The Journal of Chemical Physics](#) **83**, 6071 (1985); doi: 10.1063/1.449597

View online: <http://dx.doi.org/10.1063/1.449597>

View Table of Contents: <http://scitation.aip.org/content/aip/journal/jcp/83/12?ver=pdfcov>

Published by the [AIP Publishing](#)

Articles you may be interested in

[Ligandfield theory applied to diatomic transition metals. Results for the d A 9 d B 92 states of Ni₂, the d Ni 9 d Cu 102 states of NiCu, and the d Ni 8\(3 F\)d Cu 102*1 excited states of NiCu](#)
J. Chem. Phys. **97**, 4641 (1992); 10.1063/1.463867

[EPR study of VO₂ + ions doped in single crystals of NH₄I and NH₄Br](#)
J. Chem. Phys. **83**, 3744 (1985); 10.1063/1.449136

[5 D 3–5 D 4 cross relaxation in Tb³⁺ pairs in CsCdBr₃ crystals](#)
J. Chem. Phys. **83**, 476 (1985); 10.1063/1.449562

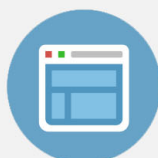
[Role of the 4f 55d band in the radiationless 5 D 15 D 0 coupling in BaCl₂:Sm²⁺ and BaBr₂:Sm²⁺](#)
J. Chem. Phys. **65**, 3108 (1976); 10.1063/1.433524

[EPR studies of NH₄Br:Cu²⁺](#)
J. Chem. Phys. **58**, 769 (1973); 10.1063/1.1679265



Re-register for Table of Content Alerts

Create a profile.



Sign up today!



Bonding in d^9 complexes derived from EPR: Application to CuCl_4^{2-} , CuBr_4^{2-} , and $\text{CdCl}_2\cdot\text{Cu}^{2+}$

J. A. Aramburu and M. Moreno

Departamento de Optica y Estructura de la Materia, Facultad de Ciencias, Universidad de Santander, 39005 Santander, Spain

(Received 20 February 1985; accepted 1 July 1985)

In this work are reported the theoretical expressions for the $[g]$, hyperfine, and superhyperfine (shf) tensors of a d^9 square-planar complex within a molecular orbital (MO) scheme. These expressions include contributions arising from crystal field and charge transfer excitations calculated up to third and second order perturbations, respectively. This makes the present framework more general than those previously used. Through those expressions we have derived from the experimental EPR and optical data the MO coefficients corresponding to the valence $b_{1g}(x^2 - y^2)$, $b_{2g}(xy)$, and $e_g(xz, yz)$ levels and also the core polarization contribution K to the hyperfine tensor for the systems CuCl_4^{2-} , CuBr_4^{2-} , and $\text{CdCl}_2\cdot\text{Cu}^{2+}$. The $3d$ charge obtained for CuCl_4^{2-} is equal to 0.61, 0.83, and 0.85 for the antibonding $3b_{1g}$, $2b_{2g}$, and $2e_g$ levels, respectively. These figures are much closer to the $X\alpha$ results by Bencini and Gatteschi [J. Am. Chem. Soc. **105**, 5535 (1983)] than to those by Desjardins *et al.* [J. Am. Chem. Soc. **105**, 4590 (1983)]. The σ and π covalency for CuBr_4^{2-} are both higher than for CuCl_4^{2-} in accord to the lower electronegativity for bromine. However, only for the antibonding $3b_{1g}$ level of CuBr_4^{2-} have we obtained an electronic charge lying mainly on ligands. The covalency of $\text{CdCl}_2\cdot\text{Cu}^{2+}$ is smaller than that found for CuCl_4^{2-} , a fact associated to a higher metal–ligand distance for the former. Evidence of this statement are also given from the analysis of crystal-field spectra and isotropic shf constant. The values of K derived for CuCl_4^{2-} ($128.1 \times 10^{-4} \text{ cm}^{-1}$), CuBr_4^{2-} ($103.6 \times 10^{-4} \text{ cm}^{-1}$), and $\text{CdCl}_2\cdot\text{Cu}^{2+}$ ($123.9 \times 10^{-4} \text{ cm}^{-1}$) point out the dependence of K on the equatorial covalency but also on the existence of axial ligands. The $[g]$ tensor of CuBr_4^{2-} is dominated by the charge transfer contribution while the crystal field one is negative. Finally an analysis of the importance of each one of the involved contributions to the spin-Hamiltonian parameters is reported for the three systems, together with the results obtained through a full diagonalization within crystal field and charge transfer states.

I. INTRODUCTION

The one-electron levels of transition-metal complexes ML_n can be reasonably well described by molecular orbitals (MO) of the form

$$|\psi^j\rangle = \alpha_j |\varphi_M^j\rangle - \beta_j |\chi_L^j\rangle, \quad (1)$$

where $|\varphi_M^j\rangle$ is a metal orbital and $|\chi_L^j\rangle$ is a symmetry-adapted linear combination of valence orbitals of the involved ligands. Since the advent of EPR spectroscopy it was early recognized that the experimental spin-Hamiltonian parameters convey information on the MO coefficients α_j, β_j corresponding to a paramagnetic complex.

The values of these coefficients derived from the experimental spin-Hamiltonian parameters can however, be quite sensitive to the accuracy of the theoretical expressions employed in the analysis. This is specially true when a significant covalency is present in several one-electron levels of the complex. As regards d^9 complexes not only these MO coefficients but also the value of the core polarization contribution to the hyperfine tensor $-K$ are dependent on the quality of the theoretical expressions used in the analysis of the experimental spin-Hamiltonian parameters.

Historically Owen¹ was the first to report a theoretical expression for the $[g]$ tensor of a d^9 ion in a D_{4h} square-

planar geometry taking account, at least partially, of bonding. This attempt then is the initial one to improve the theoretical expressions founded on a pure crystal field description.^{2,3}

The basic assumptions of Owen's model are the following:

- The promotion of an electron of a filled shell to the level $3b_{1g}$ (transforming like $x^2 - y^2$) does not modify the one-electron orbitals. Briefly these orbitals remain "frozen" in the excitation process.
- A second-order (in energy) perturbation approach suffices for calculations.
- Only excitations to crystal-field states are considered.
- Ligand spin-orbit coupling is discarded.
- Covalency is only significant for the $3b_{1g}$ level.
- s - p ligand hybridization and metal–ligand overlap integrals can be neglected.

The subsequent work by Maki and McGarvey⁴ on the $[g]$ and hyperfine tensor of square-planar d^9 complexes took into account the covalency in the antibonding $2b_{2g}$ (transforming like xy) and $2e_g$ (transforming like xz, yz) levels as well as the ligand hybridization in the $3b_{1g}$ level. In a further step Kivelson and Neiman⁵ improved the expressions by

Maki and McGarvey by including the metal–ligand overlap integrals but only for the $3b_{1g}$ level. Thus in the model by Kivelson and Neiman assumptions (a) to (d) of Owen's model are kept while the remaining ones are modified. As regards the superhyperfine (shf) tensor these authors used only first order expressions and thus neglected the influence upon it of excited states coupled to the ground state via spin-orbit coupling.

The work by Lacroix and Emch⁶ on the $[g]$ tensor of d^3 and d^8 complexes stressed the importance that charge transfer excitations could also have in a correct interpretation of the spin-Hamiltonian parameters.

Following this line Smith⁷ proposed a theoretical expression for the $[g]$ tensor of a d^9 complex with square-planar geometry in which only assumptions (a) and (b) of Owen's model were retained. Thus by comparison with the corresponding expressions by Kivelson and Neiman, in those by Smith all the overlap integrals and the effects of spin-orbit coupling (on central and ligand ions) both for crystal-field and charge transfer excitations, were also taken into account.

Chow *et al.*⁸ analyzed their experimental EPR data on CuCl_4^{2-} and CuBr_4^{2-} complexes using Smith's theoretical expressions for the $[g]$ tensor but the same first-order expressions used by Kivelson and Neiman for the superhyperfine tensor. On the other hand the second-order expression derived by Chow *et al.*⁸ for the hyperfine tensor is incorrect. In fact in the calculations of matrix elements $\langle \psi^i | H_{\text{hf}} | \psi^j \rangle$ where $|\psi^i\rangle$ and $|\psi^j\rangle$ are MO orbitals [Eq. (1)] and

$$H_{\text{hf}} = 2g_N(M)\beta\beta_N \left\{ \frac{3\mathbf{r}(\mathbf{s}\cdot\mathbf{r})}{r^5} + \frac{1}{r^3} - \frac{\mathbf{s}}{r^3} \right\} \mathbf{I} \quad (2)$$

means the hyperfine coupling between the electronic spin (and \mathbf{I}) and the nuclear spin of central ion, they replace H_{hf} by the "equivalent operator" $H_{\text{hf}}(\text{eq})$:

$$H_{\text{hf}}(\text{eq}) = P \left\{ \mathbf{I}\cdot\mathbf{I} + \frac{2}{21} \left[6\mathbf{I}\cdot\mathbf{s} - \frac{3}{2}(\mathbf{I}\cdot\mathbf{I})(\mathbf{I}\cdot\mathbf{S}) - \frac{3}{2}(\mathbf{I}\cdot\mathbf{S})(\mathbf{I}\cdot\mathbf{I}) \right] \right\} \quad (3)$$

where

$$P = 2g_N(M)\beta\beta_N \langle r^{-3} \rangle_M. \quad (4)$$

In this case $\langle r^{-3} \rangle_M$ means $\langle \varphi_M^i | r^{-3} | \varphi_M^i \rangle$ where $|\varphi_M^i\rangle$ is a d function of central ion. However, this is only true provided both $|\psi^i\rangle$ and $|\psi^j\rangle$ be a *pure* d function of the central ion.⁹

Subsequent to this work the calculation of the second-order contribution to the shf tensor arising from crystal-field excitations was reported.¹⁰ It was shown that this contribution is not negligible.¹⁰

In the same line it was also noticed¹¹ that the third order contribution to the $[g]$ tensor calculated within the MO framework, is higher than that one could expect using the pure crystal-field expressions and assuming an empirical reduction factor for the metal spin-orbit coefficient. Also it was shown that this contribution may be comparable to the second-order contribution coming from charge-transfer excitations.

These facts stress that if we want to extract *reliable* information on the covalency of a given paramagnetic complex by means of EPR data it is necessary first of all to have

adequate theoretical expressions for the spin-Hamiltonian parameters. In a further step it is also convenient to analyze the relative importance of each one of the involved contributions.

In this sense the aims of the present work are the following:

(1) To provide the correct theoretical expressions for the $[g]$, hyperfine, and shf tensor of a square-planar d^9 complex including contributions up to third order for crystal field excitations and up to second order for charge transfer excitations. In this calculation ligand spin-orbit coupling, ligand hybridization, and metal–ligand overlap integrals are taken into account. The one-electron orbitals for the excited states are assumed to be the same as for the ground state. In other words only assumption (a) of Owen's model is actually kept through the present calculation.

Furthermore in order to check that the remaining higher order contributions are not significant, calculations of the spin-Hamiltonian parameters using a full diagonalization of the spin-orbit operator within crystal field and charge transfer states¹² have also been carried out.

(2) To derive from those theoretical expressions and from the experimental EPR and optical data the MO coefficients for the $3b_{1g}$, $2b_{2g}$, $2e_g$, $1b_{2g}$, $1e_g$ levels and the value of K corresponding to the square planar CuCl_4^{2-} and CuBr_4^{2-} complexes as well as to the system $\text{CdCl}_2:\text{Cu}^{2+}$.

(3) To analyze in each one of these systems the importance of all the involved contributions to the spin-Hamiltonian parameters.

The tetragonal CuCl_4^{2-} complex has received a great deal of attention in recent times.^{8,13–27} Besides the relative simplicity of its geometric and electronic structure it gives rise to several bidimensional compounds^{16–19} and also is present in the active sites of some copper proteins.²¹ Information on the covalency of this complex has been sought through theoretical $X\alpha$,^{22,23} *ab initio*,^{24,25} and extended Hückel²⁶ calculations and also from the experimental EPR and optical data.⁸ Nevertheless, the situation is not clear at present. In this sense for instance Chow *et al.*⁸ obtain that the covalency in the π antibonding $2b_{2g}$ and $2e_g$ levels is clearly higher than in the $3b_{1g}$ level which has σ character. Furthermore those authors report a higher electronic charge on the ligands than on copper for the antibonding $2e_g$ level.

The $X\alpha$ calculations by Desjardins *et al.*²² give the same $3d$ charge for $3b_{1g}$ and $2e_g$ levels. Also in these levels the electronic charge lies more on ligands than on central ion. These results are in contrast with the $X\alpha$ calculations by Bencini and Gatteschi²³ where for every one of the antibonding levels the $3d$ charge on copper is always higher than that on ligands. Also the $3d$ charge on copper is clearly higher for the antibonding $3b_{1g}$ level than for the $2e_g$ level. As regards CuBr_4^{2-} ^{8,28} no theoretical calculations on it have been reported to our knowledge and thus information on the MO coefficients is specially desirable. In this case we are particularly interested in the comparison with the results on CuCl_4^{2-} . In this sense one would expect an increase of the covalency in view of the lower electronegativity of bromine with respect to that of chlorine. However the coefficients derived by Chow *et al.*⁸ from their EPR data are against this view.

On the other hand the relative importance of each one of the involved contributions to the spin-Hamiltonian parameters could change significantly with respect to what is found in CuCl_4^{2-} due to the likely increase in covalency and also to the value of the bromine spin-orbit coefficient which is about four times higher than that of chlorine.

As far as $\text{CdCl}_2\text{:Cu}^{2+}$ is concerned²⁹⁻³² it exhibits an elongated O_h geometry rather than a true square-planar situation despite the fact that only the shf interaction due to the equatorial ligands is seen by EPR. On the other hand as the $\text{Cd}^{2+}\text{--Cl}^-$ distance is 2.74 Å it is very likely that the equatorial $\text{Cu}^{2+}\text{--Cl}^-$ distance in $\text{CdCl}_2\text{:Cu}^{2+}$ is higher than the 2.265 Å which corresponds to the tetragonal CuCl_4^{2-} complex. Effects of this kind have been recently demonstrated in some fluoroperovskites and alkali halide lattices doped with Mn^{2+} .³³ This fact which would imply changes in the equatorial covalency of the $\text{CdCl}_2\text{:Cu}^{2+}$ system with respect to that of CuCl_4^{2-} , deserves an investigation, which is also carried out in this paper.

II. THEORETICAL

A. Spin Hamiltonian

The spin Hamiltonian of a MX_4 complex ($\text{M} = d^9$ ion, $\text{X} = \text{ligand}$) neglecting quadrupolar effects is given by

$$\begin{aligned} \mathcal{H} = & \beta \{ g_{\parallel} H_z S_z + g_{\perp} (H_x S_x + H_y S_y) \} + A_{\parallel} S_z I_z \\ & + A_{\perp} (S_x I_x + S_y I_y) + \sum_{j=1}^4 \{ T_{x_j'} S_{x_j'} I_{x_j'} + T_{y_j'} S_{y_j'} I_{y_j'} \\ & + T_{z_j'} S_{z_j'} I_{z_j'} \}. \end{aligned} \quad (5)$$

The last term reflects the superhyperfine interaction, the local coordinates $\{X_j', Y_j', Z_j'\}$ being defined in Fig. 1.

B. One-electron orbitals

If one neglects in a first step the spin-orbit coupling, the MO characteristics of the antibonding $3b_{1g}$, $2b_{2g}$, $2e_g$ levels and those of the bonding $1b_{2g}$ and $1e_g$ levels, all of them corresponding to the ground state ${}^2B_{1g}$ of the complex, are defined on Table I.

These orbitals are the most important as regards the EPR properties of the MX_n complex in which the excitations

$$\Delta_1 = \epsilon(3b_{1g}) - \epsilon(2b_{2g}), \quad \Delta_2 = \epsilon(3b_{1g}) - \epsilon(2e_g),$$

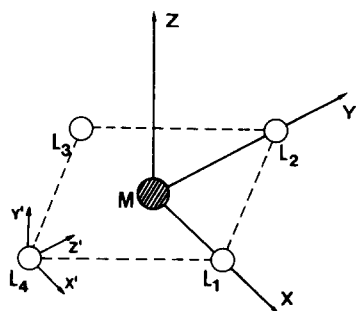


FIG. 1. The arrangement of local axis are illustrated for the L_4 ligand of the ML_4 complex.

TABLE I. Molecular orbitals characteristic of the antibonding $3b_{1g}$, $2b_{2g}$, $2e_g$ levels and of the bonding $1b_{2g}$, $1e_g$ levels.

$ 3b_{1g}\rangle = \alpha_0 d_{x^2-y^2}\rangle - \beta_0 \{ \mu \chi_{p\sigma}(b_{1g}) \rangle + (1 - \mu^2)^{1/2} \chi_s(b_{1g}) \rangle \},$
$ 2b_{2g}\rangle = \alpha_1 d_{xy}\rangle - \beta_1 \chi_{p\pi}(b_{2g}) \rangle,$
$ 2e_{g1}\rangle = \alpha_2 d_{xz}\rangle - \beta_2 \chi_{p\pi}(e_{g1}) \rangle,$
$ 2e_{g2}\rangle = \alpha_2 d_{yz}\rangle - \beta_2 \chi_{p\pi}(e_{g2}) \rangle,$
$ 1b_{2g}\rangle = \alpha'_1 d_{xy}\rangle + \beta'_1 \chi_{p\pi}(b_{2g}) \rangle,$
$ 1e_{g1}\rangle = \alpha'_2 d_{xz}\rangle + \beta'_2 \chi_{p\pi}(e_{g1}) \rangle,$
$ 1e_{g2}\rangle = \alpha'_2 d_{yz}\rangle + \beta'_2 \chi_{p\pi}(e_{g2}) \rangle,$
$ \chi_{p\sigma}(b_{1g}) \rangle = 1/2 \{ -p_x(1) + p_y(2) + p_x(3) - p_y(4) \},$
$ \chi_s(b_{1g}) \rangle = 1/2 \{ s(1) + s(2) + s(3) + s(4) \},$
$ \chi_{p\pi}(b_{2g}) \rangle = 1/2 \{ p_y(1) + p_x(2) - p_y(3) - p_x(4) \},$
$ \chi_{p\pi}(e_{g1}) \rangle = \frac{1}{\sqrt{2}} \{ p_x(1) - p_z(3) \},$
$ \chi_{p\pi}(e_{g2}) \rangle = \frac{1}{\sqrt{2}} \{ p_z(2) - p_z(4) \},$

$$\Delta'_1 = \epsilon(3b_{1g}) - \epsilon(1b_{2g}), \quad \Delta'_2 = \epsilon(3b_{1g}) - \epsilon(1e_g),$$

play a fundamental role. In the present calculation only the crystal field and charge transfer excitations are considered. One-electron transitions from $3b_{1g}$ to levels arising from 4s and 4p levels of the d^9 ion are unimportant for the present purposes. In fact they give rise to levels belonging to A_{1g} , E_u , and A_{2u} which cannot be coupled to a B_{1g} state via the angular momentum operator whose components transform as E_g and A_{2g} in D_{4h} .

The main goal of this work is to determine the values of MO coefficients defined in Table I and the value of K from the seven experimental EPR parameters defined in Eq. (4). It should be noted that in view of the orthogonality relations between one-electron levels the number of independent MO coefficients is actually four.

C. Calculation of matrix elements. Approximations

The spin-orbit coupling operator for one electron H_{SO} is taken as^{6,34}

$$\begin{aligned} H_{SO} &= H_{SO}^M + H_{SO}^L, \\ H_{SO}^M &= \xi_M(r) \mathbf{l} \cdot \mathbf{s}; \quad H_{SO}^L = \sum_{k=1}^4 \xi_L(r - r_k) \mathbf{l}_k \cdot \mathbf{s}. \end{aligned} \quad (6)$$

Here $\xi_M(r)$ corresponds to the central ion while $\xi_L(r - r_k)$ refers to the ligand placed at \mathbf{r}_k ; \mathbf{l}_k is the orbital angular momentum referred to \mathbf{r}_k as origin.

In calculating matrix elements of the form $\langle \psi | H_{SO} | \psi' \rangle$ it is assumed that $\langle \psi | H_{SO}^M | \psi' \rangle = \alpha_i \alpha_j \langle \varphi^i_M | H_{SO}^M | \varphi^j_M \rangle$. Similar approximations are used in the calculations of matrix elements $\langle \psi | H_{SO}^L | \psi' \rangle$.

The value of matrix elements like $\langle \varphi^i_M | \xi_M(r) | \varphi^j_M \rangle$, where $|\varphi^i_M\rangle$ is a d function of the central ion, is made equal to ξ_M . This quantity is actually quite close to the spin-orbit coefficient of the free ion. Its value can be determined taking into account the true charge on central ion in the complex. In the same way the value of matrix elements like $\langle p_z(i) | \xi_L(r - r_i) | p_z(i) \rangle = \xi_L$ can be derived from the spin-orbit coefficient of L^0 and L^{-1} ions ($L = \text{halide}$).

The preceding approximations are all of them founded on the dependence of $\xi_M(r)$ and $\xi_L(r - r_k)$ on r and its valid-

ity has been verified by several authors.^{6,34,35}

The unpaired electron gives rise to an anisotropic hyperfine contribution and at the same time *induces* an isotropic contribution via the core polarization. For calculating the first contribution we have also assumed that

$$\langle \psi^i | H_{\text{hf}} | \psi^j \rangle = \alpha_i \alpha_j \langle \varphi_M^i | H_{\text{hf}} | \varphi_M^j \rangle. \quad (7)$$

Here H_{hf} is the operator given by Eq. (2), and the matrix elements $\langle \varphi_M^i | H_{\text{hf}} | \varphi_M^j \rangle$ can now be easily calculated using the equivalent operator⁹ given in Eq. (3).

In the case of the superhyperfine interaction where the core polarization contribution plays a very minor role³⁶ the calculations of matrix elements have been carried out on the same grounds as for the hyperfine interactions. In this case however we have also considered the contributions arising from matrix elements like $\langle \varphi_M^i | H_{\text{shf}} | \varphi_M^j \rangle$ or $\langle \varphi_M^i | H_{\text{shf}} | p_z^j(j) \rangle$ where

$$H_{\text{shf}} = 2g_N(L)\beta\beta_N \sum_{k=1}^4 \mathbf{I}_k \left\{ \frac{1}{|\mathbf{r} - \mathbf{r}_k|^3} - \frac{\mathbf{s}}{|\mathbf{r} - \mathbf{r}_k|^3} - \frac{3(\mathbf{r} - \mathbf{r}_k)[\mathbf{s}(\mathbf{r} - \mathbf{r}_k)]}{|\mathbf{r} - \mathbf{r}_k|^5} + \frac{8\pi}{3} \mathbf{s} \cdot \delta(\mathbf{r} - \mathbf{r}_k) \right\}. \quad (8)$$

The first order contribution to the shf tensor arising from matrix elements $\langle \varphi_M^i | H_{\text{shf}} | \varphi_M^j \rangle$ has been considered explicitly by some authors. It will be shown however that in the cases analyzed through this paper the role of that contribution is small.

D. Theoretical expressions

1. g tensor

The two components of the $[g - g_0]$ tensor ($g_0 = 2.0023$) are written as a sum of three contributions

$$\begin{aligned} g_{\parallel} - g_0 &= \Delta^2 g_{\parallel}(\text{CF}) + \Delta^2 g_{\parallel}(\text{CT}) + \Delta^3 g_{\parallel}(\text{CF}), \\ g_{\perp} - g_0 &= \Delta^2 g_{\perp}(\text{CF}) + \Delta^2 g_{\perp}(\text{CT}) + \Delta^3 g_{\perp}(\text{CF}). \end{aligned} \quad (9)$$

Here $\Delta^2 g_{\parallel}(\text{CF})$ means the second order contribution arising from crystal field levels while $\Delta^2 g_{\parallel}(\text{CT})$ is the corresponding one coming from charge transfer levels. The meaning of $\Delta^3 g_{\parallel}(\text{CF})$ is thus clear. The expressions for each one of these contributions have been previously reported¹¹ and are the following,

$$\begin{aligned} \Delta^2 g_{\parallel}(\text{CF}) &= 8\alpha_0^2 \alpha_1^2 q_1 K_1 \xi_M / \Delta_1; \\ \Delta^2 g_{\perp}(\text{CF}) &= 2\alpha_0^2 \alpha_2^2 q_2 K_2 \xi_M / \Delta_2; \\ \Delta^2 g_{\parallel}(\text{CT}) &= 8\alpha_0^2 \alpha_1^2 q_1' K_1' \xi_M / \Delta_1'; \\ \Delta^2 g_{\perp}(\text{CT}) &= 2\alpha_0^2 \alpha_2^2 q_2' K_2' \xi_M / \Delta_2'; \\ \Delta^3 g_{\parallel}(\text{CF}) &= -4\alpha_0^2 \alpha_1^2 \alpha_2^2 q_2 K_1 q(1,2) \frac{\xi_M^2}{\Delta_1 \Delta_2} \\ &\quad - \alpha_0^2 \alpha_2^4 q_2^2 K(2,2) \frac{\xi_M^2}{\Delta_2^2} \\ &\quad - g_0 \alpha_0^2 \alpha_2^2 q_2^2 \frac{\xi_M^2}{\Delta_2^2}, \\ \Delta^3 g_{\perp}(\text{CF}) &= -2\alpha_0^2 \alpha_1^2 \alpha_2^2 q_1 \{q(1,2)K_2 - q_2 K(1,2)\} \frac{\xi_M^2}{\Delta_1 \Delta_2} \end{aligned} \quad (10)$$

$$\begin{aligned} &- 2g_0 \alpha_0^2 \alpha_1^2 q_1^2 \frac{\xi_M^2}{\Delta_1^2} \\ &- \left\{ \frac{g_0}{2} \alpha_0^2 \alpha_2^2 q_2^2 - \alpha_0^2 \alpha_2^4 q_2 K_2 \right\} \frac{\xi_M^2}{\Delta_2^2}, \end{aligned}$$

where

$$\begin{aligned} K_1 &= 1 - \frac{\beta_0}{\alpha_0} S_0 - \frac{\beta_1}{2\alpha_1} \left\{ 2S_1 + \frac{\beta_0}{\alpha_0} \Gamma(\mu) \right\}, \\ K_2 &= 1 - \frac{\beta_0}{\alpha_0} S_0 - \frac{\beta_2}{\sqrt{2}\alpha_2} \left\{ \sqrt{2}S_2 + \frac{\beta_0}{\alpha_0} \Gamma(\mu) \right\}, \\ K_1' &= 1 - \frac{\beta_0}{\alpha_0} S_0 + \frac{\beta_1'}{2\alpha_1'} \left\{ 2S_1 + \frac{\beta_0}{\alpha_0} \Gamma(\mu) \right\}, \\ K_2' &= 1 - \frac{\beta_0}{\alpha_0} S_0 + \frac{\beta_2'}{\sqrt{2}\alpha_2'} \left\{ \sqrt{2}S_2 + \frac{\beta_0}{\alpha_0} \Gamma(\mu) \right\}, \\ K(1,2) &= 1 + \frac{\beta_1 \beta_2}{\sqrt{2}\alpha_1 \alpha_2} - \frac{\beta_1}{\alpha_1} S_1 - \frac{\beta_2}{\alpha_2} S_2, \\ q_1 &= 1 - \frac{\beta_0 \beta_1 \mu \xi_L}{2\alpha_0 \alpha_1 \xi_M}; \quad q_2 = 1 - \frac{\beta_0 \beta_2 \mu \xi_L}{\sqrt{2}\alpha_0 \alpha_2 \xi_M}, \\ q_1' &= 1 + \frac{\beta_0 \beta_1' \mu \xi_L}{2\alpha_0 \alpha_1' \xi_M}; \quad q_2' = 1 + \frac{\beta_0 \beta_2' \mu \xi_L}{\sqrt{2}\alpha_0 \alpha_2' \xi_M}, \\ q(1,2) &= 1 + \frac{\beta_1 \beta_2 \xi_L}{\sqrt{2}\alpha_1 \alpha_2 \xi_M}. \end{aligned} \quad (11)$$

$\Gamma(\mu)$ is given by

$$\Gamma(\mu) = \mu - (1 - \mu^2)^{1/2} R \left\langle s(1) \left| \frac{\partial}{\partial y(1)} \right| p_y(1) \right\rangle \quad (12)$$

and S_0 , S_1 , and S_2 are the group overlap integrals

$$\begin{aligned} S_0 &= \mu S_{p\sigma} + (1 - \mu^2)^{1/2} S_s, \\ S_{p\sigma} &= \langle d_{x^2-y^2} | \chi_{p\sigma}(b_{1g}) \rangle; \quad S_s = \langle d_{x^2-y^2} | \chi_s(b_{1g}) \rangle, \\ S_1 &= \langle d_{xy} | \chi_{p\pi}(b_{2g}) \rangle; \quad S_2 = \langle d_{xz} | \chi_{p\pi}(e_g) \rangle. \end{aligned} \quad (13)$$

When no covalency is considered the preceding expressions lead to those by Bleaney *et al.*³ calculated in the framework of the crystal field model.

2. Hyperfine tensor

In a similar way the theoretical contributions to A_{\parallel} and A_{\perp} are decomposed as follows

$$\begin{aligned} A_{\parallel} &= -K + A_{\parallel}^1 + A_{\parallel}^2(\text{CF}) + A_{\parallel}^2(\text{CT}) + A_{\parallel}^3(\text{CF}), \\ A_{\perp} &= -K + A_{\perp}^1 + A_{\perp}^2(\text{CF}) + A_{\perp}^2(\text{CT}) + A_{\perp}^3(\text{CF}), \end{aligned} \quad (14)$$

where

$$\begin{aligned} A_{\parallel}^1 &= -\frac{4}{7} \alpha_0^2 P; \quad A_{\perp}^1 = \frac{2}{7} \alpha_0^2 P, \\ A_{\parallel}^2(\text{CF}) &= \left\{ 8\alpha_0^2 \alpha_1^2 q_1 \frac{\xi_M}{\Delta_1} + \frac{6}{7} \alpha_0^2 \alpha_2^2 q_2 \frac{\xi_M}{\Delta_2} \right\} P, \\ A_{\perp}^2(\text{CF}) &= \frac{11}{7} \alpha_0^2 \alpha_2^2 q_2 \frac{\xi_M}{\Delta_2} P, \\ A_{\parallel}^2(\text{CT}) &= \left\{ 8\alpha_0^2 \alpha_1^2 q_1' \frac{\xi_M}{\Delta_1'} + \frac{6}{7} \alpha_0^2 \alpha_2^2 q_2' \frac{\xi_M}{\Delta_2'} \right\} P, \end{aligned}$$

$$\begin{aligned}
A_{\perp}^2(\text{CT}) &= \frac{11}{7} \alpha_0^2 \alpha_2'^2 q_2' \frac{\xi_M}{\Delta_2'} P, \\
A_{\parallel}^3(\text{CF}) &= \alpha_0^2 \left\{ \frac{4}{7} (\alpha_0^2 \alpha_1^2 - \alpha_1^4) q_1^2 \frac{\xi_M^2}{\Delta_1^2} + \frac{2}{7} \left(\frac{3}{2} \alpha_2^4 \right. \right. \\
&\quad \left. \left. + \alpha_0^2 \alpha_2^2 q_2 - 4 \alpha_2^4 q_2 \right) q_2 \frac{\xi_M^2}{\Delta_2^2} - 2 \left[2q(1,2)q_2 \right. \right. \\
&\quad \left. \left. + \frac{3}{7} q_1 q_2 + \frac{3}{7} q_1 q(1,2) \right] \alpha_1^2 \alpha_2^2 \frac{\xi_M^2}{\Delta_1 \Delta_2} \right\} P, \\
A_{\perp}^3(\text{CF}) &= \alpha_0^2 \left\{ -\frac{2}{7} (\alpha_0^2 \alpha_1^2 + \alpha_1^4) q_1^2 \frac{\xi_M^2}{\Delta_1^2} - \frac{1}{14} (2\alpha_0^2 \alpha_2^2 q_2 \right. \\
&\quad \left. - 11 \alpha_2^4 q_2 \frac{\xi_M^2}{\Delta_2^2} + \frac{11}{7} [q_2 - q(1,2)] \right. \\
&\quad \left. \times \alpha_0^2 \alpha_1^2 \alpha_2^2 q_1 \frac{\xi_M^2}{\Delta_1 \Delta_2} \right\} P.
\end{aligned} \quad (15)$$

As for the $[g]$ tensor the preceding expressions lead to those derived by Bleaney *et al.*³ when covalency is fully ignored.

3. Superhyperfine tensor

As regards the shf tensor each one of the components is decomposed as follows

$$T_{x_i'} = T_{x_i'}^1 + T_{x_i'}^2(\text{CF}) + T_{x_i'}^2(\text{CT}) + T_{x_i'}^3(\text{CF}) + \delta T_{x_i'}^1. \quad (16)$$

The first-order contribution is given by the well-known expressions

$$T_{x'}^1 = A_s + 2A_p; \quad T_{x'}^1 = T_{y'}^1 = A_s - A_p, \quad (17)$$

where

$$\begin{aligned}
A_s &= \frac{\beta_0^2(1-\mu^2)}{4} A_s^0; \quad A_p = \frac{\beta_0^2\mu^2}{4} A_p^0, \\
A_s^0 &= \frac{8\pi}{3} g_0 g_N(L) \beta \beta_N |\psi_s(0)|^2, \\
A_p^0 &= \frac{2}{5} g_0 g_N(L) \beta \beta_N \langle r^{-3} \rangle_L.
\end{aligned} \quad (18)$$

The contribution $T_{x_i'}^2(\text{CF})$ was already reported¹⁰ and is given by

$$\begin{aligned}
T_{x'}^2(\text{CF}) &= \frac{2}{5} \left(\frac{3t_1}{80} + \frac{3t_2}{20\sqrt{2}} \right) A_p^0, \\
T_{x'}^2(\text{CF}) &= -\frac{2}{5} \left(\frac{3t_1}{80} + \frac{t_2}{2\sqrt{2}} \right) A_p^0, \\
T_{x'}^2(\text{CF}) &= -\frac{2}{5} \left(\frac{t_1}{8} + \frac{3t_2}{20\sqrt{2}} \right) A_p^0,
\end{aligned} \quad (19)$$

where t_1 and t_2 are defined by

$$\begin{aligned}
t_1 &= 8\alpha_0\alpha_1\beta_0\beta_1\mu q_1 \frac{\xi_M}{\Delta_1}, \\
t_2 &= 2\alpha_0\alpha_2\beta_0\beta_2\mu q_2 \frac{\xi_M}{\Delta_2}.
\end{aligned} \quad (20)$$

It should be noted that at this level of approximation the x' and y' axis are no more equivalent.

The corresponding contribution due to charge transfer excitations is as follows:

$$\begin{aligned}
T_{x'}^2(\text{CT}) &= -\frac{2}{5} \left(\frac{3t_1'}{80} + \frac{3t_2'}{20\sqrt{2}} \right) A_p^0, \\
T_{x'}^2(\text{CT}) &= \frac{2}{5} \left(\frac{3t_1'}{80} + \frac{t_2'}{2\sqrt{2}} \right) A_p^0, \\
T_{y'}^2(\text{CT}) &= \frac{2}{5} \left(\frac{t_1'}{8} + \frac{3t_2'}{20\sqrt{2}} \right) A_p^0,
\end{aligned} \quad (21)$$

where t_1' and t_2' are defined by

$$\begin{aligned}
t_1' &= 8\alpha_0\alpha_1'\beta_0\beta_1'\mu q_1' \frac{\xi_M}{\Delta_1'}, \\
t_2' &= 2\alpha_0\alpha_2'\beta_0\beta_2'\mu q_2' \frac{\xi_M}{\Delta_2'}.
\end{aligned} \quad (22)$$

The contribution $T_{x_i'}^3(\text{CF})$ is given by

$$\begin{aligned}
T_{x'}^3(\text{CF}) &= \alpha_0^2 \alpha_1^2 q_1^2 \frac{\xi_M^2}{\Delta_1^2} \left\{ -A_s - 2A_p + \frac{1}{4} \beta_1^2 A_p^0 \right\} \\
&\quad + \alpha_0^2 \alpha_2^2 q_2^2 \frac{\xi_M^2}{\Delta_2^2} \left\{ -\frac{1}{2} A_s - A_p \right. \\
&\quad \left. + \frac{1}{8} \beta_2^2 A_p^0 \right\} + \frac{3\sqrt{2}}{32} \alpha_2^2 t_2 \\
&\quad \times A_p^0 \frac{\xi_M}{\Delta_2} + \frac{5}{4} \alpha_0 \alpha_1 \alpha_2 \frac{\xi_M^2}{\Delta_1 \Delta_2} A_p^0 \\
&\quad \times \left\{ -\frac{3}{10} \alpha_2 \beta_0 \beta_1 \mu q_2 q(1,2) \right. \\
&\quad \left. - \frac{3\sqrt{2}}{10} \alpha_1 \beta_0 \beta_2 \mu q(1,2) q_1 \right. \\
&\quad \left. + \sqrt{2} \alpha_0 \beta_1 \beta_2 q_1 q_2 \right\}, \\
T_{x'}^3(\text{CF}) &= \alpha_0^2 \alpha_1^2 q_1^2 \frac{\xi_M^2}{\Delta_1^2} \left\{ -A_s + A_p - \frac{1}{2} \beta_1^2 A_p^0 \right\} \\
&\quad + \alpha_0^2 \alpha_2^2 q_2^2 \frac{\xi_M^2}{\Delta_2^2} \left\{ -\frac{1}{2} A_s + \frac{1}{2} A_p \right. \\
&\quad \left. - \frac{1}{8} \beta_2^2 A_p^0 \right\} - \frac{5\sqrt{2}}{16} \alpha_2^2 t_2 A_p^0 \\
&\quad \times \frac{\xi_M}{\Delta_2} + \frac{5}{4} \alpha_0 \alpha_1 \alpha_2 \frac{\xi_M^2}{\Delta_1 \Delta_2} A_p^0 \\
&\quad \times \left\{ \frac{3}{10} \beta_0 \beta_1 \mu \alpha_2 q(1,2) q_2 \right. \\
&\quad \left. - \frac{3\sqrt{2}}{10} \alpha_0 \beta_1 \beta_2 q_1 q_2 - \sqrt{2} \alpha_1 \beta_0 \beta_2 \mu q_1 q(1,2) \right\}, \\
T_{y'}^3(\text{CF}) &= \alpha_0^2 \alpha_1^2 q_1^2 \frac{\xi_M^2}{\Delta_1^2} \left\{ -A_s + \frac{5}{2} A_p \right. \\
&\quad \left. - \frac{1}{4} \beta_2^2 A_p^0 \right\} + \alpha_0^2 \alpha_2^2 q_2^2 \frac{\xi_M^2}{\Delta_2^2}
\end{aligned} \quad (23)$$

$$\begin{aligned} & \times \left\{ -\frac{1}{2}A_s + \frac{1}{2}A_p - \frac{1}{4}\beta_2^2 A_p^0 \right\} \\ & - \frac{3\sqrt{2}}{16} \alpha_2^2 t_2 A_p^0 \frac{\xi_M}{\Delta_2} \\ & + \frac{5}{4} \alpha_0 \alpha_1 \alpha_2 \frac{\xi_M^2}{\Delta_1 \Delta_2} \left\{ \beta_0 \beta_1 \mu \alpha_2 q(1,2) q_2 \right. \\ & + \frac{3\sqrt{2}}{10} \beta_0 \beta_2 \mu \alpha_1 q_1 q(1,2) \\ & \left. - \frac{3\sqrt{2}}{10} \alpha_0 \beta_1 \beta_2 q_1 q_2 \right\} A_p^0. \end{aligned}$$

Finally the contribution termed $\delta T_{x_i}^1$ arises from metal-metal and metal-ligand matrix elements and can be written as

$$\begin{aligned} \delta T_{x'}^1 &= 2(A_D + A_{ML}), \\ \delta T_{x''}^1 &= \delta T_{y'}^1 = -(A_D + A_{ML}). \end{aligned} \quad (24)$$

We have verified that the metal-metal contribution A_D is well approximated by

$$A_D = \alpha_0^2 g_0 g_N(L) \beta \beta_N / R^3. \quad (25)$$

The metal-ligand contribution A_{ML} is obtained calculating numerically

$$\begin{aligned} A_{ML} &= -\frac{1}{2} \alpha_0 \beta_0 \{ \mu \langle d_{x^2-y^2} | H_D^1 | p_x(1) \rangle \\ &+ (1 - \mu^2)^{1/2} \langle d_{x^2-y^2} | H_D^1 | s(1) \rangle \}, \end{aligned} \quad (26)$$

where

$$H_D^1 = g_0 g_N(L) \beta \beta_N \frac{3z'^2 - r'^2}{r'^5} \quad (27)$$

and $r' = |\mathbf{r} - \mathbf{r}_1|$.

III. APPLICATIONS

A. Atomic parameters

Atomic parameters like ξ_M or $\langle r^{-3} \rangle_M$ which enter the theoretical expressions given in the preceding section depend, though very slightly, on the charge on central ion. Owing to this in this work we have assumed $3d$ and $4s$ charges on copper equal to $9.5e$ and $0.5e$ for all the studied systems. These values are close to those calculated by Benicini *et al.*²³ for CuCl_4^{2-} . From these figures we have derived the following parameters for copper, chlorine, and bromine by an extrapolation of experimental³⁷ and theoretical^{38,39} results

$$\begin{aligned} \xi_M &= 790 \text{ cm}^{-1}; \quad \langle r^{-3} \rangle_M = 53.4 \times 10^{24} \text{ cm}^{-3}, \\ \xi_L &= 515 \text{ cm}^{-1}; \quad |\psi_{3s}(0)|^2 = 69.4 \times 10^{24} \text{ cm}^{-3} \text{ (chlorine)}, \\ \xi_L &= 2200 \text{ cm}^{-1}; \quad |\psi_{4s}(0)|^2 = 126.3 \times 10^{24} \text{ cm}^{-3} \text{ (bromine)}. \end{aligned}$$

The Hartree-Fock value, $\langle r^{-3} \rangle_{\text{hf}}$, for $\langle r^{-3} \rangle_{3p}$ of Cl^- is $38.8 \times 10^{24} \text{ cm}^{-3}$ which is 15% smaller than the corresponding value $\langle r^{-3} \rangle_{\text{hf}} = 45.7 \times 10^{24} \text{ cm}^{-3}$ for atomic chlorine, denoted as Cl^0 .

The dipolar hyperfine interaction between the elec-

tronic and nuclear spins has been measured in Cl^0 . These data stress⁴⁰ that the true value, termed $\langle r^{-3} \rangle_s$, for Cl^0 is 1.17 higher than $\langle r^{-3} \rangle_{\text{hf}}$, a fact which is due to configuration interaction effects. Similar results have also been obtained for fluorine and oxygen atoms.⁴¹

Thus accepting that the ratio $\langle r^{-3} \rangle_s / \langle r^{-3} \rangle_{\text{hf}}$ is independent of the ligand charge and equal to 1.17 we derive for a chlorine ion with a charge of $-0.70e$ a value $\langle r^{-3} \rangle_{3p} = 47.7 \times 10^{24} \text{ cm}^{-3}$ which is practically the same as $\langle r^{-3} \rangle_{\text{hf}}$ for Cl^0 .

In the analysis of the shf tensor of paramagnetic complexes the difference between $\langle r^{-3} \rangle_s$ and $\langle r^{-3} \rangle_{\text{hf}}$ has usually been ignored. Moreover the $\langle r^{-3} \rangle_{\text{hf}}$ value corresponding to the atom rather than that of the anion has been commonly used in the interpretation of the shf tensor of paramagnetic complexes. The preceding arguments now explain the validity of such a procedure in the case of chlorine.⁴²

Since for bromine $\langle r^{-3} \rangle_s$ has not been measured we also assume $\langle r^{-3} \rangle_s / \langle r^{-3} \rangle_{\text{hf}} = 1.17$. As $\langle r^{-3} \rangle_{\text{hf}} = 69.05 \times 10^{24} \text{ cm}^{-3}$ for Br^- and $\langle r^{-3} \rangle_{\text{hf}} = 81 \times 10^{24} \text{ cm}^{-3}$ for Br^0 , we finally obtain $\langle r^{-3} \rangle_{4p} = 84.7 \times 10^{24} \text{ cm}^{-3}$. As regards the value of $\langle ns | \partial / \partial y | np_y \rangle$, we have calculated it using the wave functions by Clementi and Roetti.³⁹ The obtained values are in agreement with the values reported by Misetich and Watson⁴³ and are practically independent on the halogen charge. These values are $\langle 3s | \partial / \partial y | 3p_y \rangle = 0.411 \text{ a.u.}$ for chlorine and $\langle 4s | \partial / \partial y | 4p_y \rangle = 0.427 \text{ a.u.}$ for bromine. Other authors have used quite different values for $\langle ns | \partial / \partial y | np_y \rangle$. In particular Smith⁷ and Chow *et al.*⁸ use values close to -0.35 a.u. for chlorine while the latter authors employ -0.55 a.u. for bromine. In s^1 systems it has been shown however, that a positive value of $\langle ns | \partial / \partial y | np_y \rangle$ allows one to understand why the most covalent systems have a positive g shift while the most ionic ones exhibit negative g shifts.⁴⁴

It is now necessary to say that if we take the parameters corresponding to free Cu^+ or Cu^{2+} instead of the present ones the change in the values of the MO coefficients derived from EPR data is not significant, a fact which supports the reliability of the method. Taking as a guide β_0 , this parameter changes by less than 5% when we use the atomic parameters of Cu^+ instead of those of Cu^{2+} .

B. Derivation of MO coefficients and K

The values of MO coefficients and K have been obtained from the experimental EPR parameters using the expressions reported in Sec. II, by means of a least-square fit procedure. For measuring the quality of fitting we use the parameter

$$w = \sum_i \left(\frac{\lambda_i^f - \lambda_i^i}{\lambda_i^i} \right)^2, \quad (28)$$

where λ_i and λ_i^f correspond to input data and fitted values, respectively.

C. Study of the square-planar CuCl_4^{2-} complex

The spin-Hamiltonian parameters for this square-planar complex were measured by Chow *et al.*⁸ in $\text{K}_2\text{PdCl}_4:\text{Cu}^{2+}$. These are the reported values,

TABLE II. Values of the MO coefficients for CuCl_4^{2-} derived in the present work. These values are compared to the extended Hückel calculations by Ros and Schuit (Ref. 27) and to the ones reported by Chow *et al.* (Ref. 8). The value of w , measuring the fitting quality is $w = 1.3 \times 10^{-3}$.

	α_0	β_0	μ	α_1	β_1	α_2	β_2	α'_1	β'_1	α'_2	β'_2
Present work	0.827	0.686	0.966	0.934	0.451	0.937	0.412	0.368	0.897	0.354	0.913
Calculated by Ros and Schuit	0.771	0.770	0.985	0.914	0.479	0.787	0.663	0.411	0.881	0.619	0.751
Derived by Chow <i>et al.</i>	0.865	0.630	0.980	0.744	0.714	0.717	0.732	0.673	0.701	0.698	0.684

$$g_{\parallel} = 2.2326 \pm 0.0002, \quad g_{\perp} = 2.049 \pm 0.002,$$

$$|A_{\parallel}| = (163.6 \pm 0.5) \times 10^{-4} \text{ cm}^{-1};$$

$$|A_{\perp}| = (34.5 \pm 0.6) \times 10^{-4} \text{ cm}^{-1},$$

$$T_z = (23.3 \pm 0.3) \times 10^{-4} \text{ cm}^{-1};$$

$$|T_{x'}| = |T_{y'}| = (5.3 \pm 1) \times 10^{-4} \text{ cm}^{-1}.$$

The crystal field transitions for this complex have been measured by Cassidy and Hitchmann.¹⁵ From their data we take $\Delta_1 = 12\,500 \text{ cm}^{-1}$ and $\Delta_2 = 14\,300 \text{ cm}^{-1}$. This assignment is supported by the calculations by Bencini and Gatteschi²³ and by those due to the Correa de Mello *et al.*²⁶ As the charge-transfer transitions $1b_{2g} \rightarrow 3b_{1g}$ and $1e_g \rightarrow 3b_{1g}$ are parity forbidden they are likely masked by the allowed $3e_u(\pi) \rightarrow 3b_{1g}$ and $2e_u(\sigma) \rightarrow 3b_{1g}$ bands which are observed experimentally and whose maxima lie at $26\,400$ and $35\,900 \text{ cm}^{-1}$, respectively.²² The calculated values for these allowed transitions are 6000 cm^{-1} smaller than the experimental ones.²² In view of this and on the calculated values for Δ'_1 and Δ'_2 by Desjardins *et al.*,²² we can take as reasonable the following values $\Delta'_1 = 38\,000 \text{ cm}^{-1}$ and $\Delta'_2 = 35\,000 \text{ cm}^{-1}$.

The value of the metal–ligand distance R has been taken $R = 2.265 \text{ \AA}$ and the corresponding values of the overlap integrals are $S_s = 0.095$, $S_{p\sigma} = 0.116$, $S_1 = 0.090$, and $S_2 = 0.063$. The values of the best MO coefficients derived from the experimental EPR data for CuCl_4^{2-} by means of the expressions given in Sec. II are collected on Table II and compared to the results given by other authors for the same system. In this derivation we have taken the experimental A_{\parallel} and A_{\perp} values as being both negative while the experimental $T_1 = T_{x'} = T_{y'}$ value has been taken as positive. Other choices of signs lead to meaningless results.

On Table III are reported the values of the electronic charge density distribution for the antibonding $3b_{1g}$, $2b_{2g}$, and $2e_g$ levels obtained by a Mulliken analysis. These values are compared to those coming from two recent $X\alpha$ calculations. Finally in Table IV is reported the values of the individual contributions to the spin-Hamiltonian parameters, the value of K and also a comparison of the best “theoretical” values with the experimental ones. In this table the results obtained through a full diagonalization procedure are included as well. Our results on CuCl_4^{2-} shown in Tables II and III indicate that (i) the covalency is indeed higher for the σ -level $3b_{1g}$ than for the other antibonding $2b_{2g}$ and $2e_g$ levels, which have a π character. (ii) In the three antibonding

levels the electronic charge is higher on copper than on the four ligands. These conclusions are at variance with the data reported by Chow *et al.*⁸ and also with the $X\alpha$ calculation by Desjardins *et al.*²² Our data are, however, very close to the theoretical values by Bencini and Gatteschi²³ (Table III). The comparison between the “calculated” spin-Hamiltonian parameters and the corresponding experimental ones, shown in Table IV, is satisfactory, specially if we consider that we have fitted five independent parameters to six independent experimental data by means of our theoretical expressions. On the other Table IV points out that, for the present case, the perturbative approach employed throughout this work for calculating the spin-Hamiltonian parameters gives accurate results. As regards the $[g - g_0]$ tensor of CuCl_4^{2-} , it is shown in Table IV that none of the three involved contributions is negligible. In this case $\Delta^2g(\text{CF})$ is dominant with respect to $\Delta^2g(\text{CT})$, while the latter is also more important than $\Delta^3g(\text{CF})$.

The present analysis gives a value of the core polarization contribution $K = 128.1 \times 10^{-4} \text{ cm}^{-1}$ which is indeed nearly twice the value $K = 68 \times 10^{-4} \text{ cm}^{-1}$ calculated by Bencini and Gatteschi.²³ Owing to this and to the use of approximate expressions for A_{\parallel} and A_{\perp} , these authors were unable to explain satisfactorily the experimental hyperfine tensor of CuCl_4^{2-} . In addition our value $K = 128.1 \times 10^{-4}$

TABLE III. Charge density (in %) for the antibonding $3b_{1g}$, $2b_{2g}$, and $2e_g$ levels of the ground state of CuCl_4^{2-} compared to the calculations by: (a) Bencini and Gatteschi (Ref. 23) and (b) Desjardins *et al.* (Ref. 22).

	Cu	Cl	inter + outer sphere	
Present work	61	39	...	
(a)	56	37	7	$3b_{1g}$
(b)	42	49	9	
Present work	83	17	...	
(a)	80	16	4	$2b_{2g}$
(b)	60	31	9	
Present work	85	15	...	
(a)	73	24	4	$2e_g$
(b)	40	48	12	

TABLE IV. Values of the different contributions to the $[g]$, hyperfine and shf tensors for the square-planar CuCl_4^{2-} complex. The hyperfine and shf tensors are given in 10^{-4} cm^{-1} units.

	$\Delta^2g(\text{CF})$	$\Delta^2g(\text{CT})$	$\Delta^3g(\text{CF})$	Total	Full diagonalization	Experimental values
$g_{\parallel} - g_0$	0.1955	0.0410	-0.0086	0.2279	0.2260	0.2303 ± 0.0002
$g_{\perp} - g_0$	0.0376	0.0150	-0.0072	0.0454	0.0452	0.047 ± 0.002

	$-K$	A^1	$A^2(\text{CF})$	$A^2(\text{CT})$	$A^3(\text{CF})$	Total	Full diagonalization	Experimental values
A_{\parallel}	-128.1	-149.5	110.0	10.9	-3.8	-160.5	-161.3	-163.6 ± 0.5
A_{\perp}	-128.4	75.1	15.9	2.7	-0.2	-35.0	-35.0	-34.5 ± 0.6

	T^1	$T^2(\text{CF})$	$T^2(\text{CT})$	$T^3(\text{CF})$	δT^1	Total	Full diagonalization	Experimental values
T_x	21.7	0.7	-0.4	0.2	0.38	22.5	22.2	23.3 ± 0.3
T_x'	6.1	-1.3	0.9	-0.2	-0.16	5.4	5.6	5.3 ± 1
T_y	6.1	-1.8	0.9	-0.1	-0.16	5.1	5.1	5.3 ± 1

cm^{-1} is close to $K = 130 \times 10^{-4} \text{ cm}^{-1}$ derived theoretically from free Cu^{2+} .⁴⁵ As regards the shf tensor, Table IV shows that $T^2(\text{CF})$ and $T^2(\text{CT})$, which are usually neglected, are more important than δT^1 , and can be up to 30% of the experimental value in the case of the T_x and T_y components. Nevertheless, there is a great deal of cancellation between $T^2(\text{CF})$ and $T^2(\text{CT})$, which minimizes their total influence upon the shf tensor. In spite of this fact the present analysis predicts that $T_x > T_y$.

This point cannot be verified from the data reported by Chow *et al.*⁸ However, Kubo *et al.* have recently measured by NMR the hyperfine fields on Cl nuclei in $(\text{CH}_3\text{NH}_3)_2\text{CuCl}_4$.²⁰ From this work the shf tensor for this system can be derived to be $T_x = (23.2 \pm 0.2) \times 10^{-4} \text{ cm}^{-1}$, $T_x' = (5.87 \pm 0.2) \times 10^{-4} \text{ cm}^{-1}$, $T_y = (4.38 \pm 0.2) \times 10^{-4} \text{ cm}^{-1}$, which is indeed quite similar to that previously reported by Chow *et al.*⁸ for $\text{K}_2\text{PdCl}_4\text{:Cu}^{2+}$. These data indicate that T_x is indeed higher than T_y though the difference $T_x - T_y = (1.5 \pm 0.4) \times 10^{-4} \text{ cm}^{-1}$ is higher than that obtained from Table IV.

In our analysis of the shf tensor of CuCl_4^{2-} we have discarded the contribution due to the core polarization on the ligand. This contribution K_L can be *roughly estimated* as being equal to $\beta_0^2 A_{cp}^0 / 4$ where $A_{cp}^0 = 11 \times 10^{-4} \text{ cm}^{-1}$ corresponds to free Cl^0 atom.⁴¹ Taking β_0 from Table II we find $K_L \approx 1 \times 10^{-4} \text{ cm}^{-1}$. This figure means that core polarization on ligands plays a very minor role in the shf tensor, at variance with the importance of the core polarization in the hyperfine tensor.

D. Study of $\text{CdCl}_2\text{:Cu}^{2+}$

The low temperature EPR spectrum of $\text{CdCl}_2\text{:Cu}^{2+}$ is characteristic of a static Jahn-Teller effect. Its spin-Hamiltonian parameters have been measured by Thornley *et al.*²⁹ and more recently by Hayashi *et al.*³² The values given by the last authors are

$$\begin{aligned}
 g_{\parallel} &= 2.335 \pm 0.004, \quad g_{\perp} = 2.075 \pm 0.003, \\
 |A_{\parallel}| &= (117.5 \pm 1.4) \times 10^{-4} \text{ cm}^{-1}, \\
 |A_{\perp}| &= (13.1 \pm 0.1) \times 10^{-4} \text{ cm}^{-1}, \\
 T_z &= (20 \pm 1.3) \times 10^{-4} \text{ cm}^{-1}.
 \end{aligned}$$

Similar values were found by Thornley *et al.*^{29,46} who give $|T_{\parallel}| = |T_x| = |T_y| = (5.0 \pm 0.5) \times 10^{-4} \text{ cm}^{-1}$.

Accepting these values for $\text{CdCl}_2\text{:Cu}^{2+}$ we notice significant differences with respect to the values for the square planar CuCl_4^{2-} complex, especially in the case of the hyperfine tensor. This is also true when we compare the corresponding crystal field transitions. In this connection, Kan'no *et al.*³¹ observed three $d-d$ bands in $\text{CdCl}_2\text{:Cu}^{2+}$ peaked at 6372, 9437, and $10\,970 \text{ cm}^{-1}$, which should be compared to the values found for a pure tetragonal CuCl_4^{2-} complex^{13,15,23,26}: 12 500 (assigned as $2b_{2g} \rightarrow 3b_{1g}$), 14 300 (assigned as $2e_g \rightarrow 3b_{1g}$), and $16\,900 \text{ cm}^{-1}$ (assigned as $3a_{1g} \rightarrow 3b_{1g}$). We have assigned the three crystal field peaks in $\text{CdCl}_2\text{:Cu}^{2+}$ as follows: the peaks at 9437 and $10\,970 \text{ cm}^{-1}$ are $2b_{2g} \rightarrow 3b_{1g}$ and $2e_g \rightarrow 3b_{1g}$ transitions, respectively, while the remainder arises from the $3a_{1g} \rightarrow 3b_{1g}$ transition. The experimental intensity³¹ of the assigned $2e_g \rightarrow 3b_{1g}$ band is about three times higher than that of the assigned $2b_{2g} \rightarrow 3b_{1g}$ band. These values are quite similar to those found in CuCl_4^{2-} and thus support the present assignment.

The present assignment implies an equatorial $\text{Cu}^{2+} - \text{Cl}^-$ distance, R , higher than $R = 2.265 \text{ \AA}$, characteristic of the tetragonal CuCl_4^{2-} complex.¹⁴ At the same time the low value of the peak energy corresponding to the $3a_{1g} \rightarrow 3b_{1g}$ transition should be related to the existence of axial ligands¹³ in $\text{CdCl}_2\text{:Cu}^{2+}$. In this way the semiempirical model by Day⁴⁷ provides reliable predictions for the $2b_{2g} \rightarrow 3b_{1g}$ and $2e_g \rightarrow 3b_{1g}$ transitions. The experimental values of these transitions for $\text{CdCl}_2\text{:Cu}^{2+}$ are quite consistent with values of R around 2.35 \AA and of $R_{ax} \approx 2.8 \text{ \AA}$. Here R_{ax} refers to

the distance between Cu^{2+} and the axial ligands. Moreover, assuming those distances, Day's model predicts a value around 4500 cm^{-1} for the $3a_{1g} \rightarrow 3b_{1g}$ transition. Though the agreement with the experimental value is not good enough for that transition, the last figure supports the present assignment. The fact that R in $\text{CdCl}_2:\text{Cu}^{2+}$ is likely near to 2.35 \AA is also consistent with the following facts:

(i) In Cs Cu Cl_3 , Cu^{2+} is surrounded by a distorted octahedron of Cl^- ions.⁴⁸ The mean equatorial distance is $R = 2.32\text{ \AA}$ while $R_{ax} = 2.78\text{ \AA}$. In this case experimental crystal field peaks at 8300 and $10\,000\text{ cm}^{-1}$ have been assigned¹³ to arise from the $3a_{1g} \rightarrow 3b_{1g}$ and $2b_{2g} \rightarrow 3b_{1g}$ transitions, respectively.

(ii) It has been recently pointed out³³ that for ionic complexes the isotropic superhyperfine constant A_s is proportional to $S_z^2(R)$ and thus it is sensitive to the true distance between an impurity and the ligands. From the reasoning exposed in Sec. III C and the experimental shf tensor, we can expect a value $A_s = (10 \pm 0.8) \times 10^{-4}\text{ cm}^{-1}$ for $\text{CdCl}_2:\text{Cu}^{2+}$, which is smaller than the value $A_s = 11.5 \times 10^{-4}\text{ cm}^{-1}$ obtained for CuCl_4^{2-} . This again supports the idea that R is indeed higher in $\text{CdCl}_2:\text{Cu}^{2+}$ than in CuCl_4^{2-} . Furthermore, if we accept that in the present cases A_s is also proportional to $S_z^2(R)$ we obtain a value $\Delta R \approx 0.07\text{ \AA}$, where ΔR is the difference between the R values corresponding to $\text{CdCl}_2:\text{Cu}^{2+}$ and CuCl_4^{2-} . This figure then supports a value of R for $\text{CdCl}_2:\text{Cu}^{2+}$ very close to 2.35 \AA .

As regards the charge transfer excitations, Kan'no *et al.*³⁰ observed two bands in $\text{CdCl}_2:\text{Cu}^{2+}$ peaked at $25\,510\text{ cm}^{-1}$ and at $33\,874\text{ cm}^{-1}$, which can be reasonably assigned as being the allowed $3e_u(\pi) \rightarrow 3b_{1g}$ and $2e_u(\sigma) \rightarrow 3b_{1g}$ transitions by comparison with the results on CuCl_4^{2-} . Following this assignment, the two charge transfer peaks lie at an energy which is about 1500 cm^{-1} less than those for CuCl_4^{2-} . Assuming that this is also true for any other charge transfer transition, we take $\Delta'_1 = 36\,000\text{ cm}^{-1}$ and $\Delta'_2 = 33\,000\text{ cm}^{-1}$. For calculating the values of the MO coefficients shown in Table V and the value of $K = 123.9 \times 10^{-4}\text{ cm}^{-1}$ (Table VI) we have taken $R = 2.35\text{ \AA}$. For this value of R one calculates $S_{p\sigma} = 0.106$, $S_z = 0.084$, $S_1 = 0.081$, and $S_2 = 0.057$. As for CuCl_4^{2-} the signs for $A_{||}$ and A_{\perp} are taken as negative, while that of T_1 as positive. Other choices of signs lead to meaningless results.

Table V clearly shows that the covalency in the three antibonding levels of $\text{CdCl}_2:\text{Cu}^{2+}$ is somewhat smaller than that corresponding to CuCl_4^{2-} , a fact which can also be relat-

ed to the higher value of R existing in $\text{CdCl}_2:\text{Cu}^{2+}$. Generally speaking, covalency tends to decrease when the metal-ligand distance increases. This feature has been obtained in the self-consistent MO calculations on MnF_6^{4-} ^{49,50} and CrF_6^{3-} ⁵⁰ performed for several values of the metal-ligand distance. In this line also the analysis⁵² of the ENDOR data on $\text{NaCl}:\text{Ag}^0$ and $\text{KCl}:\text{Ag}^0$ reveal: (i) That the $p\sigma$ unpaired spin density on the ligand, f_σ , is 22% smaller in $\text{KCl}:\text{Ag}^0$ than in $\text{NaCl}:\text{Ag}^0$. (ii) That the difference between the $\text{Ag}^0\text{-Cl}^-$ distance in $\text{KCl}:\text{Ag}^0$ and $\text{NaCl}:\text{Ag}^0$ is about 0.3 \AA .

Table VI points out how the relative importance of the contributions to the spin-Hamiltonian parameters has changed noticeably with respect to the situation found in CuCl_4^{2-} . In this sense, for instance, $|\Delta^3 g_1(\text{CF})|$ is now higher than $\Delta^2 g_1(\text{CT})$ and $A_{||}^2(\text{CF})$ cancels out $A_{||}^1$ completely. This fact then stresses that slight changes in the MO parameters may induce more substantial changes upon the spin-Hamiltonian parameters. In the same vein it is worth noting that K in $\text{CdCl}_2:\text{Cu}^{2+}$ is only $4.5 \times 10^{-4}\text{ cm}^{-1}$ smaller than in CuCl_4^{2-} despite the great differences existing between the corresponding components of the hyperfine tensor.

Generally speaking, an increase in the covalency tends to decrease the value of K , a fact which is related to a higher $4s$ population for the central ion fostered by bonding.⁵³ The fact that K is slightly smaller for $\text{CdCl}_2:\text{Cu}^{2+}$ than for CuCl_4^{2-} in spite of the higher covalency of the latter system could be perhaps due to bonding with axial ligands in the former case. This can increase the $4s$ population in the $3a_{1g}$ level, giving rise to a smaller value of K despite the fact that the covalency in $3b_{1g}$ is indeed higher for CuCl_4^{2-} than for $\text{CdCl}_2:\text{Cu}^{2+}$.

E. Study of CuBr_4^{2-}

EPR measurements on the square-planar CuBr_4^{2-} complex were also carried out by Chow *et al.*⁸ This complex was formed in Cu^{2+} doped K_2PdBr_4 and its spin-Hamiltonian parameters are

$$g_{||} = 2.143 \pm 0.003; \quad g_{\perp} = 2.043 \pm 0.002,$$

$$|A_{||}| = (189.5 \pm 0.8) \times 10^{-4}\text{ cm}^{-1},$$

$$|A_{\perp}| = 45.8 \times 10^{-4}\text{ cm}^{-1},$$

$$T_z = (123 \pm 2) \times 10^{-4}\text{ cm}^{-1},$$

$$|T_x| = |T_y| = (27.9 \pm 1) \times 10^{-4}\text{ cm}^{-1}.$$

Though the true value of R is not known for this case we shall take $R = 2.42\text{ \AA}$ from the structural data reported by Fletcher *et al.*⁵⁴ on compounds containing square-planar CuBr_4^{2-} units. The experimental shf tensor reported for

TABLE V. Values of the MO coefficients for $\text{CdCl}_2:\text{Cu}^{2+}$ ($w = 1.9 \times 10^{-6}$) and CuBr_4^{2-} ($w = 4.1 \times 10^{-2}$) derived from the spin-Hamiltonian parameters. The results on CuCl_4^{2-} are also included for comparison purposes.

System	α_0	β_0	μ	α_1	β_1	α_2	β_2	α'_1	β'_1	α'_2	β'_2
$\text{CdCl}_2:\text{Cu}^{2+}$	0.862	0.626	0.962	0.939	0.428	0.985	0.240	0.353	0.907	0.184	0.974
CuCl_4^{2-}	0.827	0.686	0.966	0.934	0.451	0.937	0.412	0.368	0.897	0.354	0.913
CuBr_4^{2-}	0.707	0.794	0.980	0.865	0.578	0.782	0.670	0.509	0.820	0.626	0.745

TABLE VI. Values of the different contributions to the $[g]$, hyperfine, and shf tensors for $\text{CdCl}_2 \cdot \text{Cu}^{2+}$. The hyperfine and shf tensors are given in 10^{-4} cm^{-1} units.

	$\Delta^2 g(\text{CF})$	$\Delta^2 g(\text{CT})$	$\Delta^3 g(\text{CF})$	Total	Full diagonalization	Experimental values		
$g_{\parallel} - g_0$	0.3147	0.0397	-0.0212	0.3332	0.3305	0.333 ± 0.004		
$g_{\perp} - g_0$	0.0800	0.0080	-0.0149	0.0731	0.0730	0.073 ± 0.003		
	$-K$	A^1	$A^2(\text{CF})$	$A^2(\text{CT})$	$A^3(\text{CF})$	Total	Full diagonalization	Experimental values
A_{\parallel}	-123.9	-162.3	166.9	10.3	-8.6	-117.5	-118.2	-117.5 ± 1.4
A_{\perp}	-123.9	81.2	28.7	1.0	0.0	-13.0	-13.3	-13.1 ± 0.1
	T^1	$T^2(\text{CF})$	$T^2(\text{CT})$	$T^3(\text{CF})$	δT^1	Total	Full diagonalization	Experimental values
$T_{z'}$	19.1	0.8	-0.4	0.2	0.3	20.0	19.6	20 ± 1.3
$T_{x'}$	6.2	-1.2	0.7	-0.3	-0.1	5.3	5.5	5 ± 0.5
$T_{y'}$	6.2	-2.1	0.8	-0.1	-0.1	4.7	4.8	5 ± 0.5

CuBr_4^{2-} by Chow *et al.*⁸ is essentially the same than that measured on $(\text{CH}_3\text{NH}_3)_2\text{CuCl}_2\text{Br}_2$ by means of the NMR on the bromine nuclei.²⁰ This result then suggests that the $\text{Cu}^{2+}-\text{Br}^-$ distance in the last mixed complex is the same as in $\text{K}_2\text{PdBr}_4 \cdot \text{Cu}^{2+}$ rather than equal to 2.28 \AA as assumed by Kubo *et al.*²⁰ The values of the crystal field transitions for CuBr_4^{2-} have not been reported to our knowledge. Day's model⁴⁷ and also experimental observations⁵⁵ indicate that both Δ_1 and Δ_2 are about 1000 cm^{-1} smaller than for the square-planar CuCl_4^{2-} system. Therefore we shall take $\Delta_1 = 11\,500 \text{ cm}^{-1}$ and $\Delta_2 = 13\,300 \text{ cm}^{-1}$. The charge-transfer spectrum for the square-planar CuBr_4^{2-} complex has not been measured either. However, a reasonable estimation of Δ'_1 and Δ'_2 can be made by means of the results on CuCl_4^{2-} , through Jørgensen's optical electronegativity scale⁵⁶ and also taking into account the experimental charge

transfer spectra on $\text{LiCl} \cdot \text{M}^{2+}$ and $\text{LiBr} \cdot \text{M}^{2+}$ ($\text{M}^{2+}; 3d$ cation) recently reported by Hirako and Onaka.⁵⁷ Jørgensen's scale gives a decrease of $\sim 6000 \text{ cm}^{-1}$ for the energy of the first allowed charge-transfer transition when Cl^- is replaced by Br^- as ligand of a given complex. For $\text{LiCl} \cdot \text{Cu}^{2+}$ Hirako and Onaka have found two charge transfer bands peaked at $28\,150$ and $36\,200 \text{ cm}^{-1}$. These values are actually close to those observed for the square-planar CuCl_4^{2-} complex. As regards $\text{LiBr} \cdot \text{Cu}^{2+}$, three charge transfer peaks are observed⁵⁷ placed at $19\,000$, $22\,500$, and $27\,500 \text{ cm}^{-1}$. The first two peaks arise from the same electronic transition as $\text{LiCl} \cdot \text{Cu}^{2+}$ but split off essentially by the action of the more intense ligand spin-orbit coupling. These experimental results and also those obtained on other cations thus suggest that the substitution of Cl^- by Br^- decreases the energy of charge transfer peaks by around 8000 cm^{-1} . In view of this

TABLE VII. Values of the different contributions to the $[g]$, hyperfine, and shf tensors for CuBr_4^{2-} . The hyperfine and shf tensors are given in 10^{-4} cm^{-1} units.

	$\Delta^2 g(\text{CF})$	$\Delta^2 g(\text{CT})$	$\Delta^3 g(\text{CF})$	Total	Full diagonalization	Experimental values
$g_{\parallel} - g_0$	-0.0039	0.1431	0.0020	0.1411	0.1335	0.141 ± 0.003
$g_{\perp} - g_0$	-0.0130	0.0603	-0.0009	0.0464	0.0419	0.041 ± 0.002

	$-K$	A^1	$A^2(\text{CF})$	$A^2(\text{CT})$	$A^3(\text{CF})$	Total	Full diagonalization	Experimental values
A_{\parallel}	-103.6	-108.7	-7.6	42.2	2.3	-175.4	-175.8	-189.5
A_{\perp}	-103.6	54.4	9.2	12.0	-0.2	-46.6	-46.5	-45.8

	T^1	$T^2(\text{CF})$	$T^2(\text{CT})$	$T^3(\text{CF})$	δT^1	Total	Full diagonalization	Experimental values
$T_{x'}$	116.8	-1.9	-6.9	-1.2	0.5	107.2	109.4	123 ± 2
$T_{x''}$	10.2	6.0	14.6	0.0	-0.2	30.7	29.4	27.9 ± 1.0
$T_{y'}$	10.2	2.1	15.4	-0.4	-0.2	27.1	25.1	27.9 ± 1.0

we shall take $\Delta'_1 = 30\,500\text{ cm}^{-1}$ and $\Delta'_2 = 27\,500\text{ cm}^{-1}$ as reasonable values for the square-planar CuBr_4^{2-} complex, while the overlap integrals calculated for this case are $S_{\rho\sigma} = 0.104$, $S_s = 0.082$, $S_1 = 0.082$, and $S_2 = 0.058$.

The values of the MO coefficients for CuBr_4^{2-} calculated using the preceding parameters are shown on Table V. These values have been calculated assuming that A_{\parallel} and A_1 are negative while both T_x and T_y are positive. We have verified that other choices of signs lead to meaningless results; as for CuCl_4^{2-} and $\text{CdCl}_2\cdot\text{Cu}^{2+}$. Table V clearly points out that covalency in all three antibonding levels of CuBr_4^{2-} is indeed higher than the corresponding for CuCl_4^{2-} , as could be expected from the lower electronegativity of bromine. Moreover the present results indicate that for the $3b_{1g}$ level the electronic charge lies now more on the ligands (57%) than on copper (43%). However this is not true for the π -antibonding orbitals $2b_{2g}$ and $2e_g$ in which the electronic charge, on central ions is higher than that on ligands. When the latter orbitals are compared it is seen that covalency is higher for $2e_g$ than for $2b_{2g}$.

Table VII shows the value of each one of the individual contributions to the spin-Hamiltonian parameters and one can find in it surprising results. For instance the $[g - g_0]$ tensor is, in the present case, clearly dominated by the charge transfer contribution $\Delta^2g(\text{CT})$.

Furthermore, the second order contribution from crystal field levels $\Delta^2g(\text{CF})$, which is always positive in the crystal field framework and also in that by Kivelson and Neimann,⁵ can be seen to be negative in the present case for both $\Delta^2g_{\parallel}(\text{CF})$ and $\Delta^2g_1(\text{CF})$ components. Moreover $|\Delta^2g_1(\text{CF})|$ is 4.1 times higher than $|\Delta^2g_{\parallel}(\text{CF})|$. The factors which make possible this strange situation are q_1 and q_2 which appear in the theoretical expressions for $\Delta^2g_{\parallel}(\text{CF})$ and $\Delta^2g_1(\text{CF})$ [Eq. (13)].

Concerning the hyperfine tensor we see from Table VII that in the present case the main contributions to it are, K , A^1 , and $A^2(\text{CT})$. The value of $K = 103.6 \times 10^{-4}\text{ cm}^{-1}$ obtained for the present case is smaller than $K = 128.4 \times 10^{-4}\text{ cm}^{-1}$ derived for CuCl_4^{2-} in this work. This is consistent with the view that for a given kind of complex if we keep the geometry and the central $3d$ -cation and replace the ligand by a less electronegative one, the value of the core polarization contribution K tends to decrease. It should be remarked here that K in CuBr_4^{2-} is smaller than for CuCl_4^{2-} though both $|A_{\parallel}|$ and $|A_1|$ are higher for the first complex. This fact clearly points out that a careful and simultaneous analysis of all the spin-Hamiltonian parameters of a d^9 complex is in general necessary for deriving a reliable value of the core polarization contribution K , from the experimental A_{\parallel} and A_1 values.

It should be noted however that the agreement between our "theoretical" values and the experimental ones is not so good as for CuCl_4^{2-} . In this sense for instance the calculated values for A_{\parallel} and T_x are about 10% less than the corresponding experimental values.

As regards the shf tensor it is also predicted that the in-plane shf component T_x is indeed higher than T_y . From the NMR results by Kubo *et al.* on bromine nuclei²⁰ of $(\text{CH}_3\text{NH}_3)_2\text{CuCl}_2\text{Br}_2$ it is obtained $T_x = (29.6 \pm 0.4)$

$\times 10^{-4}\text{ cm}^{-1}$; $T_y = (22.4 \pm 0.4) \times 10^{-4}\text{ cm}^{-1}$. These values are in agreement with that prediction though the difference $T_x - T_y = (7.2 \pm 0.8) \times 10^{-4}\text{ cm}^{-1}$ is higher than that obtained from Table VII.

A novel feature which appears in this case concerning the shf tensor is that $T^2(\text{CF})$ and $T^2(\text{CT})$ contributions do not cancel to as great an extent as in CuCl_4^{2-} but rather they have the same sign. This fact is also related to the negative value of q_1 and q_2 quantities in the present case which make that t_1 and t_2 have an opposite sign to that in CuCl_4^{2-} .

At variance with the results on CuCl_4^{2-} and $\text{CdCl}_2\cdot\text{Cu}^{2+}$ we see that, in the present case, the differences between the values of the spin-Hamiltonian parameters obtained through the perturbative approach and those obtained through the full diagonalization procedure are not negligible for some of the parameters. This is particularly relevant for the $g_1 - g_0$ quantity as shown in Table VII.

IV. CONCLUSIONS. FINAL REMARKS

The MO coefficients for three d^9 complexes with D_{4h} symmetry have been derived by the present method and the results are in fact reasonable.

In this line the covalency for each one of the three antibonding levels $3b_{1g}$, $2b_{2g}$, and $2e_g$ of CuBr_4^{2-} is higher than those corresponding to CuCl_4^{2-} . This is consistent with the lower electro-negativity of bromine.

On the other hand the equatorial covalency in $\text{CdCl}_2\cdot\text{Cu}^{2+}$ is smaller than in CuCl_4^{2-} a fact which is interpreted as being due to a higher value of the equatorial metal-ligand distance for the former system. Proofs of this have been derived from the analysis of the experimental (i) crystal-field transitions and (ii) isotropic shf constant A_s . The decrease of covalency when metal-ligand distance increases is a general trend which is obtained in the theoretical calculations⁴⁹⁻⁵¹ and also from the experimental EPR data for metal complexes.⁵²

In connection with this the EPR data on $\text{SrCl}_2\cdot\text{Cu}^{2+}$ reported by Bill⁵⁸ are practically identical to those for CuCl_4^{2-} pointing out a value of R which is $\sim 8\%$ smaller than that for the perfect lattice. This behavior is in line with those observed for Mn^{2+} ,^{33,59} Ni^{2+} ,⁶⁰ Cr^{3+} ,⁶¹ and $\text{Ag}^{0,52}$ impurities in ionic lattices.

In the three studied systems our results point out that covalency is higher in the σ -level $3b_{1g}$ than in the π levels $2b_{2g}$ and $2e_g$. This feature, which is consistent with the theoretical results for NiF_6^{4-} ⁶² or MnF_6^{4-} ^{63,50} means that our results are actually much closer to the $X\alpha$ calculation on CuCl_4^{2-} by Bencini and Gatteschi²³ than to the similar one reported by Desjardins *et al.*²² In this line also and in accord to the calculations by Bencini and Gatteschi²³ our results point out that for every one of the $3b_{1g}$, $2b_{2g}$, and $2e_g$ levels of CuCl_4^{2-} electronic charge lies mainly on copper. By contrast in CuBr_4^{2-} , where no $X\alpha$ calculations have been carried out, the present analysis indicates that for the $3b_{1g}$ level, charge lies more on ligands.

The results shown through this work illustrate that a good understanding of the experimental spin-Hamiltonian parameters in terms of a MO scheme needs one to be careful

with respect to the *quality* of the theoretical framework used in the analysis. This is particularly important for the hyperfine tensor of d^9 complexes. In fact in these cases the experimental value of core polarization of central ion is not as simple to derive as for d^5 ions (Mn^{2+} , Fe^{3+} , Cr^{3+}); it needs, in general, a simultaneous analysis of *all* the spin-Hamiltonian parameters. This comes because the isotropic hyperfine field for d^9 complexes is roughly 1/5 that for d^5 ions⁹ and comparable to A^1 and $A^2(CF)$.

The values of K obtained for the three studied systems outline that this quantity depends not only on the equatorial covalency but also it is sensitive to bonding with axial ligands. A further study on this point for several Cu^{2+} complexes is in progress.

The analysis carried out on $CuBr_4^{2-}$ stresses that an interpretation of the $[g]$ tensor based on crystal-field expressions with simple reduction factors can be quite meaningless: in this case $\Delta^2g(CT)$ is more important than $\Delta^2g(CF)$ which is negative. On the other hand it is just for $CuBr_4^{2-}$ where w is the highest. Related to this in complexes of s^1 ions (like Pb^{3+} , Tl^{2+} , or Ag^0), the $[g - g_0]$ tensor is due to charge-transfer excitations. In these cases quantitative agreement between experimental values and theoretical ones is problematic.⁴⁴ Perhaps the "frozen orbitals" approximation is not good enough for describing charge-transfer excitations while it is much better for crystal-field ones.^{64,65} In this way therefore it would be attractive to analyze the CuI_4^{2-} unit, which should be more covalent than $CuBr_4^{2-}$. Unfortunately the data on $NH_4I:Cu^{2+}$ ⁶⁶ indicate that in this case Cu^{2+} is two-fold rather than fourfold coordinated. Moreover no shf structure is seen in the EPR spectra. Anyway the importance of the charge-transfer excitations for explaining the positive $g_{||}$ shift of $NH_4I:Cu^{2+}$ has recently been noticed.⁶⁷

Assuming the frozen orbitals approximation, a restriction of our theoretical expressions lies on the neglect of ligand-ligand terms. The results by Smith⁷ point out however, that this neglect has in fact a small influence upon the $[g - g_0]$ tensor of several Cu^{2+} complexes.

The results of the present work point out that the perturbative procedure for deriving the MO coefficients and K is quite satisfactory for $CuCl_4^{2-}$ and $CdCl_2:Cu^{2+}$. However for $CuBr_4^{2-}$ little, but significant differences with respect to a full diagonalization calculation appear. These kinds of discrepancies will be in principle more important when ξ_M and/or ξ_L increase.

Finally we would like to comment about the phases of the molecular orbitals. We have assumed that for a pair of MO belonging to the same irreducible representation, metal and ligand orbitals are always in phase for the bonding MO and out-of-phase for the antibonding MO. It has been pointed out however, that this is not necessarily true.⁶⁸ Our choice of phases for bonding and antibonding orbitals arising from $3d$ metal levels follows SCF calculations. On the other hand the referred counterintuitive orbital mixing does not appear in frontier orbitals but in higher or lower MO.⁶⁸ We think that these arguments make our assumption reasonable.

Once the reliability of the present method for deriving K and the MO coefficients of a square-planar d^9 complex has been checked we are planning to apply it to complexes of

Ag^{2+} . These $4d^9$ complexes are likely more covalent than those corresponding to Cu^{2+} and to date no $X\alpha$ or *ab initio* calculations have been reported on them.

Note added in proof: In a very recent paper Penfield, Gewirth, and Solomon [J. Am. Chem. Soc. **107**, 4519 (1985)] also point out that the $3d$ charge density of the $3b_{1g}$ level of $CuCl_4^{2-}$ should be $\sim 61\%$ in order to explain the experimental $[g]$ tensor.

ACKNOWLEDGMENTS

Kind information by Professor R. D. Willett is acknowledged. Thanks are due to Professor L. Pueyo for sending us copies of his work prior to publication. We are also indebted to the referee by some interesting remarks. This work has been supported by the Comisión Asesora para la Investigación Científica y Técnica.

- ¹J. Owen, Proc. R. Soc. London Ser. A **227**, 183 (1955).
- ²A. Abragam and M. H. L. Pryce, Proc. R. Soc. London Ser. A **206**, 164 (1951).
- ³B. Bleaney, K. D. Bowers, and M. H. L. Pryce, Proc. R. Soc. London Ser. A **228**, 166 (1955).
- ⁴A. H. Maki and B. R. McGarvey, J. Chem. Phys. **29**, 31 (1958).
- ⁵D. Kivelson and R. Neiman, J. Chem. Phys. **35**, 149 (1961).
- ⁶R. Lacroix and G. Emch, Helv. Phys. Acta **35**, 592 (1962).
- ⁷D. W. Smith, J. Chem. Soc. A **1970**, 3108.
- ⁸C. Chow, K. Chang, and R. D. Willett, J. Chem. Phys. **59**, 2629 (1973).
- ⁹A. Abragam and B. Bleaney, *Electron Paramagnetic Resonance of Transition Ions* (Oxford University, London, 1970), p. 692.
- ¹⁰M. Moreno, J. Phys. Soc. Jpn. **53**, 1545 (1975).
- ¹¹M. Moreno, J. Phys. C **9**, 3277 (1976); Chem. Phys. Lett. **45**, 479 (1977).
- ¹²J. Aramburu and M. Moreno (unpublished work).
- ¹³D. W. Smith, Coord. Chem. Rev. **21**, 93 (1976), and references therein.
- ¹⁴R. L. Harlow, W. J. Wells, G. W. Watt, and S. H. Simonsen, Inorg. Chem. **13**, 2106 (1974).
- ¹⁵P. Cassidy and M. A. Hitchman, J. Chem. Soc. Chem. Commun. **1975**, 837.
- ¹⁶G. Heygster and W. Kleeman, Physica B **89**, 165 (1977).
- ¹⁷R. D. Willett, R. Wong, and M. Numata, J. Magn. Mater. **15**, 717 (1980).
- ¹⁸R. J. H. Wong, R. Willett, and J. E. Drumheller, J. Chem. Phys. **74**, 6018 (1981).
- ¹⁹R. D. Willett and F. Waldner, J. Appl. Phys. **53**, 2680 (1982).
- ²⁰H. Kubo, Y. Suzuki, K. Tsuru, N. Uryu, and K. Hirakawa, Mem. Fac. Eng. Kyushu Univ. **41**, 281 (1981).
- ²¹E. I. Solomon, K. W. Penfield, and D. E. Wilcox, Struct. Bond. (Berlin) **53**, 1 (1983).
- ²²S. R. Desjardins, K. W. Penfield, S. L. Cohen, R. L. Musselman, and E. I. Solomon, J. Am. Chem. Soc. **105**, 4590 (1983).
- ²³A. Bencini and D. Gatteschi, J. Am. Chem. Soc. **105**, 5535 (1983).
- ²⁴J. Demuyne and A. Veillard, Chem. Phys. Lett. **6**, 204 (1970).
- ²⁵J. Demuyne, A. Veillard, and U. Wahlgren, J. Am. Chem. Soc. **95**, 5563 (1973).
- ²⁶P. Correa de Mello, M. Hehenberger, S. Larsson, and M. Zerner, J. Am. Chem. Soc. **102**, 1278 (1980).
- ²⁷P. Ros and G. C. A. Schuit, Theor. Chim. Acta **4**, 1 (1966).
- ²⁸Y. Suzuki, K. Tsuru, Y. Kimishima, and H. Kubo, J. Phys. Soc. Jpn. **50**, 1479 (1981).
- ²⁹J. H. M. Thornley, B. W. Mangum, J. H. E. Griffiths, and J. Owen, Proc. Phys. Soc. **78**, 1263 (1961).
- ³⁰K. Kan'no, S. Naoe, S. Mukai, and Y. Nakai, Solid State Commun. **13**, 1325 (1973).
- ³¹K. Kan'no, S. Mukai, and Y. Nakai, J. Phys. Soc. Jpn. **36**, 1492 (1974).
- ³²M. Hayashi, H. Nakagawa, and H. Matsumoto, Mem. Fac. Eng. Fukui Univ. **26**, 15 (1978).
- ³³M. T. Barriuso and M. Moreno, Phys. Rev. B **29**, 3623 (1984).
- ³⁴A. A. Missetich and T. Buch, J. Chem. Phys. **41**, 2524 (1964).
- ³⁵R. Al-Mobarak and K. D. Warren, Chem. Phys. Lett. **21**, 513 (1973).
- ³⁶M. Moreno, Solid State Commun. **38**, 1045 (1981).
- ³⁷C. E. Moore, Nat. Stand. Ref. Data Ser. Nat. Bur. Stand. **35**, (1971).

- ³⁸S. Fraga, J. Karwowski, and K. M. S. Saxena, *Handbook of Atomic Data* (Elsevier, Amsterdam, 1976).
- ³⁹E. Clementi and C. Roetti, *At. Data Nucl. Data Tables* **14**, 177 (1974).
- ⁴⁰K. A. Uslu, R. F. Code, and J. S. M. Harvey, *Can. J. Phys.* **52**, 2135 (1974).
- ⁴¹J. S. M. Harvey, *Proc. R. Soc. London Ser. A* **285**, 581 (1965).
- ⁴²In the second order contributions to the shf tensor there is a part of it which arises from the coupling between the electronic orbital and the nuclear spin. The measurements on the free atom reveal that the corresponding $\langle r^{-3} \rangle_1$ value is smaller than $\langle r^{-3} \rangle_s$, which corresponds to the dipolar coupling between electronic and nuclear spins. For Cl^0 $\langle r^{-3} \rangle_s / \langle r^{-3} \rangle_1 = 1.1$. We have discarded this difference in the theoretical expressions for $T_{x_1^2}^2(\text{CF})$ and $T_{x_1^2}^2(\text{CT})$.
- ⁴³A. A. Missetich and R. E. Watson, *Phys. Rev.* **143**, 335 (1966).
- ⁴⁴M. Moreno, *Phys. Status Solidi B* **96**, 647 (1979); *Chem. Phys. Lett.* **76**, 597 (1980).
- ⁴⁵R. E. Watson and A. J. Freeman, *Hyperfine Interactions* (Academic, New York, 1967).
- ⁴⁶Thornley *et al.* (Ref. 29) have estimated $|A_1| = (0 \pm 4) \times 10^{-4} \text{ cm}^{-1}$. In the present analysis we have taken the value $|A_1| = (13.1 \pm 0.1) \times 10^{-4} \text{ cm}^{-1}$, reported by Hayashi *et al.*³²
- ⁴⁷P. Day, *Proc. Chem. Soc. London* **18**, (1964).
- ⁴⁸Y. Tazuke, H. Tanaka, K. Iio, and K. Nagata, *J. Phys. Soc. Jpn.* **50**, 3919 (1981).
- ⁴⁹J. Emery and J. C. Fayet, *Solid State Commun.* **42**, 683 (1982).
- ⁵⁰L. Pueyo (private communication).
- ⁵¹Z. Barandiaran and L. Pueyo, *J. Chem. Phys.* **80**, 1597 (1984).
- ⁵²M. T. Barriuso and M. Moreno, *Phys. Rev. B* **26**, 2271 (1982).
- ⁵³E. Simanek and K. A. Muller, *J. Phys. Chem. Solids* **31**, 1027 (1970).
- ⁵⁴R. Fletcher, J. J. Hansen, J. Livermore, and R. D. Willett, *Inorg. Chem.* **22**, 330 (1983).
- ⁵⁵R. D. Willett (private communication).
- ⁵⁶C. K. Jørgensen, *Progr. Inorg. Chem.* **12**, 101 (1970).
- ⁵⁷S. Hirako and R. Onaka, *J. Phys. Soc. Jpn.* **51**, 1255 (1982).
- ⁵⁸H. Bill, *Phys. Lett. A* **44**, 101 (1973).
- ⁵⁹M. T. Barriuso and M. Moreno, *Chem. Phys. Lett.* **112**, 165 (1984).
- ⁶⁰M. T. Barriuso and M. Moreno, *Solid State Commun.* **51**, 335 (1984).
- ⁶¹G. Fernandez-Rodrigo, L. Pueyo, M. Moreno, and M. T. Barriuso, *Phys. Rev. B* (in press).
- ⁶²A. J. H. Wachters and W. C. Nieuwpoort, *Phys. Rev. B* **5**, 4291 (1972).
- ⁶³O. Matsuoka, *J. Phys. Soc. Jpn.* **28**, 1296 (1970).
- ⁶⁴M. Florez, L. Seijo, and L. Pueyo, *Phys. Rev. B* (in press).
- ⁶⁵T. F. Soules, J. W. Richardson, and D. V. Vaught, *Phys. Rev. B* **3**, 2186 (1971).
- ⁶⁶P. Chand and G. C. Upreti, *Chem. Phys. Lett.* **88**, 309 (1982); **91**, 240 (1982).
- ⁶⁷M. Moreno and J. A. Aramburu, *Chem. Phys. Lett.* **108**, 513 (1984).
- ⁶⁸M. Whangbo and R. Hoffmann, *J. Chem. Phys.* **68**, 5498 (1978).